

Article

Energy Recovery from Municipal Solid Waste through Co-Gasification Using Steam or Carbon Dioxide with Olive By-Products

Despina Vamvuka * and Petros Tsilivakos

School of Mineral Resources Engineering, Technical University of Crete, 73100 Chania, Greece; ptsilivakos@tuc.gr

* Correspondence: vamvuka@mred.tuc.gr

Abstract: The valorization of untreated municipal waste (MSW) biochar for energetic uses, through its co-gasification with olive stone (OST) biochar under a steam or carbon dioxide atmosphere, was investigated. The experiments were conducted in a fixed bed unit and a thermal analysis–mass spectrometer system. The thermal behavior, reactivity, conversion, product gas composition, syngas yield and energy potential were determined, while the influence of the fuel’s internal structure, chemical functional groups and operating conditions were examined. The concentrations of H₂ and CO₂ in the product gas mixture under a steam atmosphere were increased with steam/biochar ratio, while that of CO was reduced. At a steam/biochar = 3 H₂ yield, the higher heating value and conversion for the OST were 52.8%, 10.8 MJ/m³ and 87.5%; for the MSW, they were 44.4%, 9.9 MJ/m³ and 51.5%, whereas for their blend, they were 50%, 10.6 MJ/m³ and 76.6%, respectively. Under a carbon dioxide atmosphere, the reactivity and conversion of the OST biochar (84%) were significantly higher as compared with the MSW biochar (50%). The higher heating value of the product gas was 12.4–12.9 MJ/m³. Co-gasification of the MSW with OST (in proportions 30:70) resulted in the enhanced reactivity, conversion, syngas yield and heating value of product gas compared with gasification of solely MSW material.

Keywords: municipal solid wastes; olive by-products; gasification



Citation: Vamvuka, D.; Tsilivakos, P. Energy Recovery from Municipal Solid Waste through Co-Gasification Using Steam or Carbon Dioxide with Olive By-Products. *Energies* **2024**, *17*, 304. <https://doi.org/10.3390/en17020304>

Academic Editor: Frede Blaabjerg

Received: 24 November 2023

Revised: 11 December 2023

Accepted: 17 December 2023

Published: 8 January 2024



Copyright: © 2024 by the authors. Licensee MDPI, Basel, Switzerland. This article is an open access article distributed under the terms and conditions of the Creative Commons Attribution (CC BY) license (<https://creativecommons.org/licenses/by/4.0/>).

1. Introduction

The amount of municipal solid waste (MSW), which is generated by virtually every activity in modern society, is continuously rising around the world due to the growth of the population and urbanization. About 2 billion tons of MSW is produced each year worldwide [1]. The high costs of land application and the environmental and health problems of this kind of disposal, caused by leaching of hazardous pollutants into the groundwater and emissions of toxic gases and dust into the atmosphere [2], are motivating effective sustainable management strategies for this waste as an alternative to deposition. The policies of the European Union and most other countries foster a reduction in MSW landfilling, according to recycling and reuse [3]. In view of the global energy crisis nowadays and the circular economy, energy recovery from these wastes, achieving the above goals, is a highly promising solution. Its direct and permanent availability, zero cost and high content in organic materials make MSW a potential feedstock for sustainable energy via waste-to-energy conversion processes.

Although the range of urban organic waste that could contribute to energy consumption worldwide varies between 1 and 3 EJ/y [4], its diverse composition, unlike other biomass materials, may create technical and environmental barriers in energy applications [5]. MSW is a combination of waste, such as food, plastics, paper, woody materials, fabrics, etc., holding high moisture, volatiles and ash deriving from dirt or soil, with a significant heavy metal content [6–8]. All these components fluctuate greatly from district to district and their characteristics may lead to slagging/fouling phenomena from ash, tar

problems and a low heating value, making its exploitation for energy purposes a difficult task. The high compositional variation of MSW requires it to be blended with higher-quality residues in order to obtain an improved feedstock configuration for energy systems. As such, agricultural woody waste, abundantly found in most countries (especially those of South Europe), with low moisture and ash, a higher heating value and a carbon-neutral footprint in the environment, seem advantageous for co-processing [9,10]. In Greece, agricultural residues possess a high potential (~3.8 Mtoe), with olive by-products accounting for about 70% [4,10].

Thermal treatment techniques not only reduce the volume of waste but also recover energy in a more environmentally favorable way than landfilling [2]. The gasification of waste materials instead of incineration, which generates several harmful pollutants, including dioxins [11], is an environmentally friendly technology [12,13]; at the same time, it offers higher efficiency and flexibility in the feedstock and end-products [13–15]. The syngas produced can be used for heat or power generation, as well as for the synthesis of biofuels and chemical substances [10,14,16–18]. When the gasification process—with either steam or carbon dioxide from a residual stream to minimize the greenhouse gas effect used as the gasifying agent—is combined with a pre-pyrolysis step, the reactivity of the charcoal is increased, and operational or downstream tar problems are eliminated [10,13,19–23].

The effectiveness of the process depends on many factors, such as the feedstock composition, gasifier type and operating conditions. A higher specific surface area [14] and inherent alkali or alkaline earth metals [6,13,21,24,25] have been found to increase the reactivity of the char. Silicon and aluminum have been claimed to have an inhibitory effect [6,26], whereas a higher amount of steam or a higher temperature have been reported to enhance the hydrogen production and calorific value of the syngas [20,27,28].

Past research on the gasification of MSW is limited throughout the literature. Most investigations have performed experiments using air as the gasifying medium, which produces a low-heating-value gas [26,29–32]. For example, the co-gasification of MSW with pine sawdust or switchgrass in air showed that by increasing the proportion of agricultural or forest biomass, the hydrogen fraction in the product stream increased, whereas that of carbon monoxide decreased, recording a higher heating value of the gas at 6.7 MJ/m³ and at a blending ratio of 40% MSW [11,33]. Others considered a single-component or model MSW composition, to avoid complications owing to feed heterogeneity [26,34]. Some researchers studied the steam gasification of MSW using catalysts and found that calcium-based catalysts showed a good capacity for carbon dioxide adsorption or tar reduction [35,36]. However, there is a lack of information on MSW co-gasification with olive by-products. In one study [37], the effect of the waste-to-polymer ratio on the yield of the MSW gasification products was investigated for various concentrations of carbon dioxide. In addition to the authors of [38], the reactivities of char samples from components of MSW to carbon dioxide were characterized by other investigators [15,26] as part of a wider study into the gasification behavior of waste streams. On the other hand, a mixture of carbon dioxide and steam was used [35] to determine the characteristics of hydrogen and syngas formation as a function of temperature, and it was found that the H₂ and CO yield increased when the CO₂/H₂O_v ratio was 0.5–2.5. Concerning olive by-products, the kinetics of steam gasification have been calculated [39,40] by performing thermogravimetric analysis experiments. More recently, olive kernels were gasified under pure CO₂ or 10% H₂O_v/He in a fixed bed [10]. The optimum performance was obtained for the slowly pyrolyzed samples, as compared to the torrefied ones.

Based on the above discussion, the current study aims to investigate the valorization of untreated municipal wastes for energetic uses, through their co-gasification with olive stones, under a steam or carbon dioxide atmosphere. The experiments were conducted in a fixed bed unit and a thermal analysis–mass spectrometer system. Thermal behavior, reactivity, conversion, product gas composition, syngas yield and energy potential were determined, and the influence of fuel internal structure, chemical functional groups and operating conditions were examined.

2. Experimental Procedures

2.1. Raw Materials and Characterization

The agro-industrial waste studied in this work, olive stone (OST), was provided by an olive mill factory, ABEA, while MSW consisting of food waste and some woody materials was collected every month during a whole year from the solid waste management company DEDISA, both located in West Crete. MSW average composition was 50% food waste materials, 30% paper, 12% woody wastes, and 8% inerts and other materials. Glasses, metals and plastic had been removed by shredding, magnetic separation and sieving by the industry for recycling. Following air drying and riffing, raw materials were ground in a cutting mill to a particle size below 1 mm. Fuel characterization of representative samples in terms of proximate analysis, ultimate analysis and calorific value was performed according to CEN/TC335 European standards [41]. For proximate analysis, high-temperature programmable furnaces were used in order to determine moisture, volatile materials and the content of ashes. For ultimate analysis, an analyzer model Flash 2000 CHNS was employed, whereas for the measurement of calorific value, a bomb calorimeter, model Leco AC-300, was used.

2.2. Biochar Production by Pyrolysis and Characterization

Pyrolysis of biomass samples was carried out in a stainless steel, fixed-bed reactor system, described in detail by the authors in a previous investigation [21]. A stainless steel basket with a rod supported the sample. The reactor was surrounded by a high-temperature furnace, with a controller of ± 3 °C accuracy. After flushing the reactor with nitrogen for 30 min, the temperature was set by the furnace controller to 600 °C and monitored by a Ni-Cr-Ni thermocouple in contact with the sample bed. The heating rate was 10 °C/min, retention time at the final temperature was 30 min and flow rate of nitrogen was 150 mL/min. Pyrolysis gases were continuously passed through salt–ice baths to collect condensable volatiles and, after reactor cooling under nitrogen, a mass balance was performed.

Biochars were characterized as before, following the CEN/TC335 standards, whereas those destined for carbon dioxide gasification tests were ground to a particle size below 200 μm in order to conduct the experiments in a kinetic regime. Structural characteristics were determined by applying the BET method to liquid nitrogen adsorption data, at relative pressures of 0.03–0.3. Samples were out-gassed overnight under vacuum in a Nova 2200 analyzer (Quantachrome) before being measured. An FTIR (Fourier-Transform Infrared) spectrophotometer, model Spectrum 1000 (Perkin Elmer), was employed for the characterization of the chemical functional groups of biochars at wave numbers 400–4000 cm^{-1} with a resolution of 4 cm^{-1} . The samples were mixed with KBr at a weight ratio of 1/100 and pelletized for the tests. A blend of OST and MSW biochars was prepared at a mass ratio of 70:30, taking into consideration the low quality of MSW, requiring a higher quality material for improving the gasification performance.

2.3. Gasification Experiments

2.3.1. Under Steam

Gasification experiments of the samples under steam were carried out in the fixed bed unit. Following charging of each biochar (5 g) in the reactor, the system was sealed, introduced into the furnace and flushed with nitrogen to eliminate air for 30 min as before. Then, it was pre-heated at 600 °C under nitrogen, at which temperature-distilled water was injected through an automatic syringe pump, passed through a 2 m pipe inside the furnace to obtain a uniform flow of steam and continued through the biochar bed. The steam-to-biochar ratio ranged between 1 and 3 for current tests. Final gasification temperature was 850 °C, heating rate was 10 °C/min and retention time was 1 h to assure complete conversion. Product gas was cooled down and dried via a cold trap and a silica gel filter, respectively. Sampling was conducted periodically using a PTFE Luer Lock special gas syringe. The results reported below are the average of replicates conducted to evaluate their reproducibility.

2.3.2. Under Carbon Dioxide

Gasification experiments of the samples under carbon dioxide were carried out in a differential thermogravimetric analyzer (TG/DTG Perkin Elmer; sensitivity < 5 µg, temperature precision ±2 °C). Particle size was below 200 µm in order to conduct the experiments under a chemical reaction control. The flow rate of carbon dioxide was 35 mL/min, the flow rate of purge gas was 45 mL/min, the heating rate was 10 °C/min and the final gasification temperature was 1000 °C. The analyzer continuously recorded the mass of each sample during heating; the derivative weight and the corresponding thermograms were also processed and evaluated. Gas analysis was conducted online, as described below. The reproducibility of the tests was high, as expressed by the relative standard deviation (RSD) reported below.

2.3.3. Gas Analysis

For the qualitative and quantitative analysis of product gases, a quadrupole mass spectrometer (MS QME-200 Balzers), coupled online with the thermogravimetric analyzer, was used. The transfer line (fused silicon capillary i.d. 0.32 mm, encased with a stainless steel sheath) was heated to 200 °C to prevent condensation of species, whereas high-purity argon with flow rate 35 mL/min was used as the purge gas. Detection of ions, which were separated in terms of their mass-to-charge ratio (m/z), was performed by a secondary electron multiplier (SEM) operating at 82 eV within an atomic mass range of 1–400, and data processing was performed by Pyris v.3.5 and Quadstar 422 software. A series of TG/MS experiments with calcium oxalate monohydrate of varying mass was carried out in order to check and confirm the flow stability and the linearity of the capillary response by comparison of the DTG and MS profiles. Calibration factors were calculated using high purity gases in argon, taking into consideration the intensity of fragments from the compounds analyzed at each m/z ratio. Calibration factors for CO, CO₂ and H₂O were also determined from the experiments with calcium oxalate monohydrate.

3. Results

3.1. Physical and Chemical Characteristics of Raw Materials and Biochars

Table 1, comparing the proximate and ultimate analyses of raw fuels and biochars, shows that the content of volatiles of raw materials was high, while that of the MSW sample represented most of the organic matter. The lower carbon and hydrogen contents of MSW, in conjunction with its higher amount of ash, resulted in a lower heating value. The concentration of sulfur in both fuels was very low; however, that of nitrogen was considerable, implying possible toxic emissions during thermal processing.

Table 1. Proximate and ultimate analyses of raw fuels and biochars (% dry).

Sample	Volatile Matter	Fixed Carbon	Ash	C	H	N	O	S	HHV (MJ/kg)
Raw fuels									
OST	73.9	18.8	7.3	49.5	6.3	2.0	34.6	0.3	19.9
MSW	73.4	0.9	25.7	38.5	5.9	1.5	28.1	0.3	16.7
Biochars									
OST	-	76.7	23.3	60.8	1.8	1.7	12.4	-	20.8
MSW	-	49.8	50.2	33.8	1.0	1.4	13.6	-	10.4

The yield of biochar was higher for OST, which was enriched in carbon and minerals after decomposition of H- and O- bearing organic compounds, implying the development of stable aromatic structures. On the other hand, the carbon content of MSW was reduced upon pyrolysis and the higher heating value decreased accordingly, suggesting that carbon was bound in volatile species in this case.

The specific surface area of both fuels, one of the principal factors affecting the reactivity of the materials during the gasification process [14,16], increased after evolution of the volatile species (Figure 1). For OST, the increase with respect to the raw material was about five-fold, while for MSW, this was about 95-fold. Nevertheless, these values were quite low, most probably associated with the high ash content of biochars, which could prevent the access of pyrolytic gas to the pores [19].

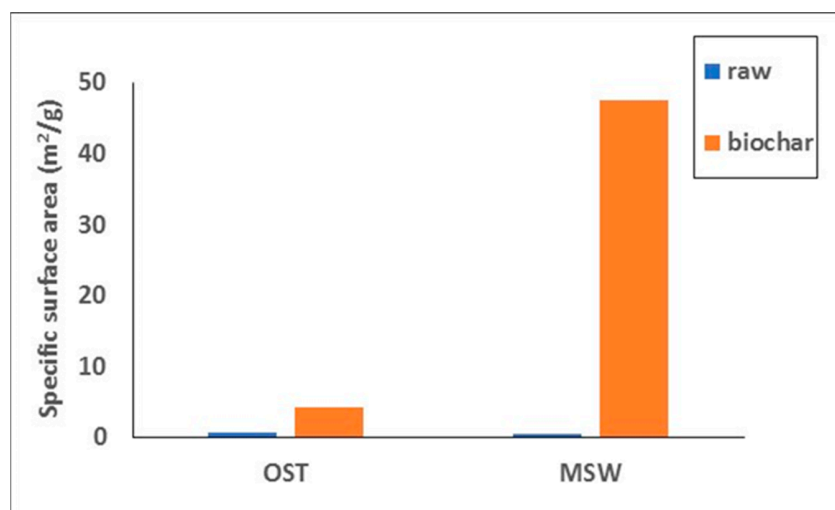


Figure 1. Specific surface area of fuels.

The chemical functional groups of devolatilized samples, identified from the FTIR spectra (Figures A1 and A2, Appendix A) obtained at wave numbers of 400–4000 cm⁻¹, are represented in Table 2. The small peaks at wavelengths of 700–900 cm⁻¹ are attributed to C-H stretching vibration from substituted benzene derivatives. The broad bands at 1006 cm⁻¹ and 1017 cm⁻¹ are assigned to C=C, C—O and C—N groups, characteristic of alkenes, alcohols, and ethers and amines, respectively. Small peaks obtained for OST at 1626 cm⁻¹ and for MSW at 1798 cm⁻¹ correspond to C=C bending vibrations of cyclic alkenes and C-H/C=O aromatic compounds, respectively. The sharp peak obtained at 1398 cm⁻¹ and 1420 cm⁻¹ and the smaller peak at 2517 cm⁻¹ are characteristic of —OH bending vibration from alcohols or carboxylic acids. On the other hand, the absence of bands above 1650 cm⁻¹ for OST biochar, corresponding to aliphatic, hydroxyl or carboxyl functional groups, indicates the higher aromaticity of this fuel in comparison with MSW after heat treatment [42], also confirmed by the ultimate analysis shown above.

Table 2. Chemical functional groups of biochars.

Chemical Functional Groups	Wave Number (cm ⁻¹)	
	OST	MSW
700–880	704	715
C-H substituted benzene	832	880
	876	
1000–1020		
C=C alkenes, C-O alcohols/ethers, C-N amines	1006	1017
1400–1440		
OH alcohols, carboxylic acids	1398	1420
1566–1650		
C=C cyclic alkene	1626	
1785–1815		
C=O, C-H aromatic compounds		1798
2500–3300		
OH carboxylic acids		2517

3.2. Gasification under Steam

During endothermic gasification reactions, temperature is very important for the increased conversion and composition of product gas. Table 3 shows these variations, by keeping the steam/biochar ratio constant. When the temperature increased from 650 °C to 850 °C, the concentration of hydrogen in the product mixture rose from 45.1% mol to 52.8% mol for OST, whereas it rose from 35.6% mol to 44.4% mol for MSW. On the other hand, the concentration of carbon monoxide was reduced from 39.2% mol to 31% mol for OST and from 41.4% mol to 29.5% mol for MSW, respectively. Taking into consideration that carbon dioxide was also enriched in the product gas, reactions (2) and (5) presented below were favored in this case.

Table 3. Effect of temperature on composition of gas and higher heating value at steam/biochar = 3 (% dry).

Sample	Temperature (°C)	H ₂	CH ₄	CO ₂	CO	C _x H _y	HHV (MJ/kg)
(mol %)							
OST	650	45.1	1.0	14.7	39.2	0.05	11.2
	700	48.4	1.1	15.3	35.2	0.05	11.1
	750	48.5	1.0	15.7	34.7	0.05	11.0
	800	48.9	1.0	16.2	33.8	0.05	11.0
	850	52.8	0.14	16.0	31.0	0.06	10.8
MSW	650	35.6	0.9	22.0	41.4	0.05	10.2
	700	39.2	0.9	23.2	36.6	0.05	10.1
	750	39.7	1.0	23.8	35.4	0.05	10.0
	800	40.5	1.0	25.0	33.4	0.05	9.9
	850	44.4	1.0	25.1	29.5	0.05	9.9

Methane and light hydrocarbons were produced in small amounts. As conversion of fuels was low at temperatures below 800 °C, in order to investigate the optimum distribution of gases of the fuels studied in terms of syngas production and its higher heating value, the steam/biochar ratio was varied between 1 and 3. The results at 850 °C are depicted in Figure 2. At steam/biochar = 1, the product gas mixture was enriched in CO followed by H₂, lower quantities of CO₂ and minor quantities of CH₄ and hydrocarbons. According to the principal reactions taking place under an atmosphere of steam, presented below, reactions (1), (3) and (5) were dominant in this case. As the steam/biochar ratio increased up to 3, the concentrations of H₂ and CO₂ rose, while that of CO dropped, agreeing with earlier data [8,36]. Therefore, under a high steam flow, endothermic reactions (1) and (2) and water–gas shift reaction (5) were promoted. The nearly constant concentration of CO₂, as a function of steam/biochar ratio for MSW fuel (Figure 2b), suggests that Boudouard reaction (3) was less favored in this case. The maximum hydrogen yield, which occurred at steam/biochar = 3, at 850 °C, was 52.8% mol for OST and 44.4% for MSW (Table 3). The composition of gas mixture generated by blending OST with MSW was in between the ones corresponding to each fuel component (Figure 2c). Although in the literature there are several data on steam gasification of agricultural residues for comparison with current results, reporting hydrogen concentration in product gas to vary between 48% mol and 58% mol, and that of carbon monoxide between 15% mol and 25% mol, at steam/biochar = 3 and temperatures 800–900 °C [8,43,44], there are quite limited studies on the steam gasification of MSW. In such studies, which are noted to differ in experimental equipment and conditions used, the hydrogen and carbon monoxide contents were found to be 32–57% mol and 15–17% mol, respectively [8,36]. For experiments in air at about 800 °C, these values were found to be 7–27% mol for hydrogen and 19–33% mol for carbon monoxide [7,30].

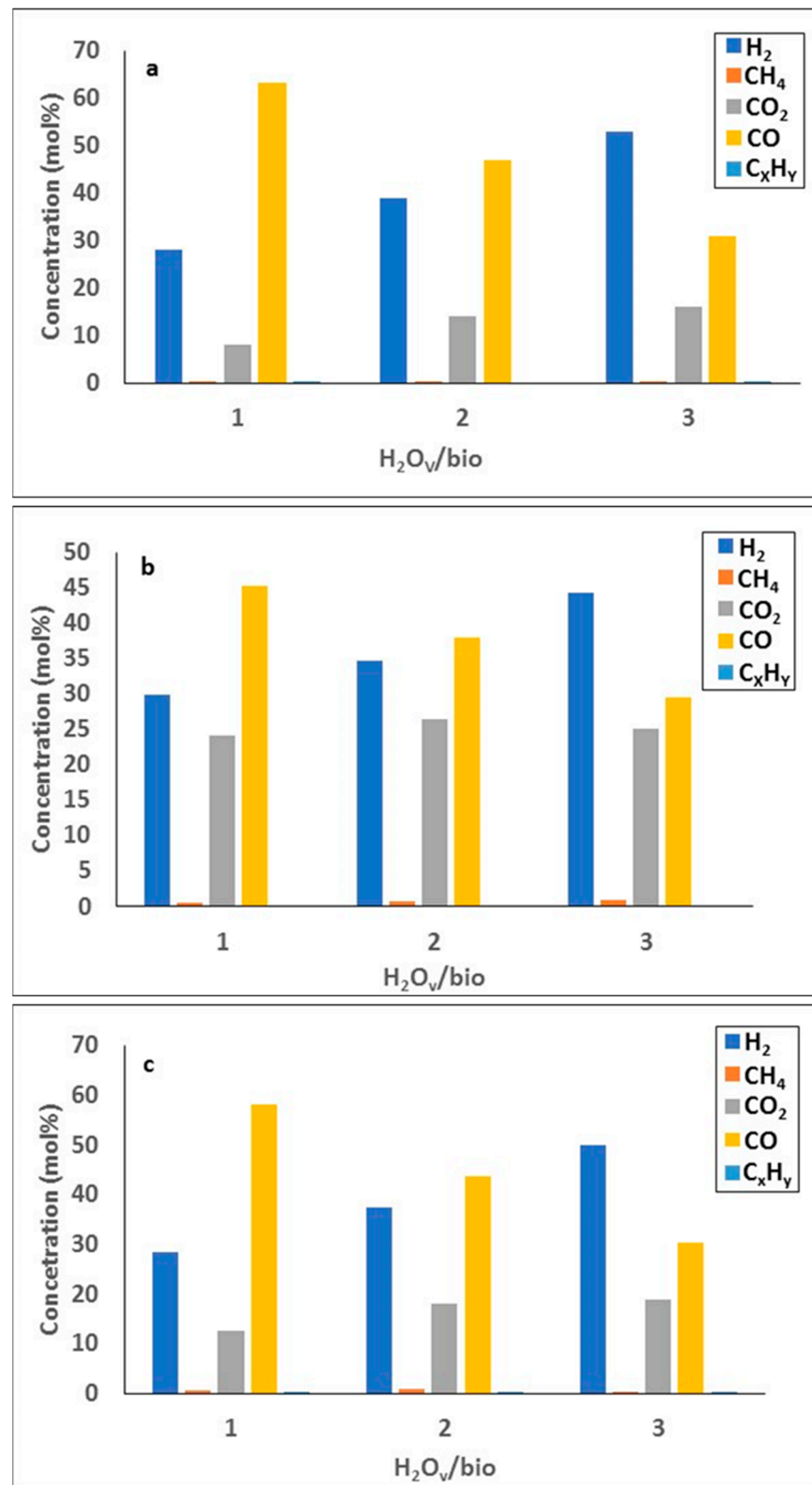
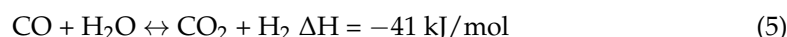
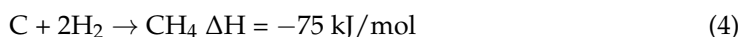
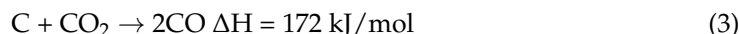


Figure 2. Composition of gas as a function of H_2O_v/bio for (a) OST, (b) MSW and (c) OST/MSW fuels.

Principal gasification reactions:





The higher heating value of product gases upon steam gasification, as a function of steam/biochar ratio, as well as final conversion and syngas yield, are exhibited in Table 4. As can be seen, when the steam/biochar ratio increased from 1 to 3, the higher heating value of OST gas decreased; this is because, as previously shown, despite the enhancement in H₂ content, CO concentration was significantly reduced. However, for MSW material, the balance between H₂, CO₂ and CO concentrations in the generated gas had a small positive effect on its higher heating value, which exceeded the value reported in literature of 8.2 MJ/m³ [34]. Co-gasification of MSW with OST resulted in a product gas with increased heating value, in comparison to that from the gasification of sole MSW material.

Table 4. Effect of steam/biochar ratio on higher heating value and final conversion.

Steam/Biochar	Higher Heating Value (MJ/m ³)			Conversion (%)			Syngas Yield (m ³ /kg)		
	OST	MSW	OST/MSW	OST	MSW	OST/MSW	OST	MSW	OST/MSW
1	11.9	9.5	11.3	75.5	40.5	64.9	0.77	0.30	0.60
2	11.0	9.6	10.7	80.8	44.9	69.8	0.82	0.33	0.63
3	10.8	9.9	10.6	87.5	51.5	76.6	1.03	0.44	0.80

Concerning conversion, Table 4 shows that a higher value was achieved for OST biochar, ranging between about 76% and 88%. Although the specific surface area was quite low for this fuel, its carbon and hydrogen contents and degree of aromatization were higher than those of MSW fuel, whereas the amount of ash was lower (Tables 1 and 2). MSW biochar, shown to consist of alcohols and carboxylic acids (Table 2), and to exhibit high ash content, presented a conversion of about 41–52%. However, when MSW was gasified together with OST, a higher conversion was achieved, ranging from 64.9% to 76.6%. The yield of syngas in Table 4 was calculated as follows:

$$Y_{\text{syn}} = x_{\text{syn}} \times V_g \text{ (m}^3\text{/kg)} \quad (7)$$

where x_{syn} is the volume fraction of syngas in the product mixture and V_g is the volume of total gas produced at 850 °C. A comparison of Figure 2 and Table 4 explains the higher syngas yield of OST, which was directly correlated to its higher conversion. Accordingly, the maximum values were obtained at steam/biochar = 3, where conversion was increased.

3.3. Gasification under Carbon Dioxide

The DTG gasification profiles of OST and MSW biochars and their mixture, under an atmosphere of carbon dioxide, are displayed in Figure 3. Table 5 summarizes the characteristic parameters derived from the processing of these profiles. As can be observed, char gasification occurred between 650 °C and 950 °C. MSW biochar, being a more heterogeneous material than the lignocellulosic OST, presented a bimodal DTG curve; decomposed earlier than OST biochar, but with a lower rate; and its maxima (T_{max}) was centered at ~805 °C. The reactivity (expressed as $R_{\text{max}}/T_{\text{max}}$) and conversion of OST biochar were significantly higher (two-fold and 84% vs. 50%, respectively). The characteristic parameters of the OST/MSW 70:30 mixture remained close to the weighted average values. The results show that when MSW was blended with the higher-quality woody fuel, OST upgraded fuels were produced, enriched in organic matter, which exhibited enhanced gasification reactivity and conversion compared to MSW.

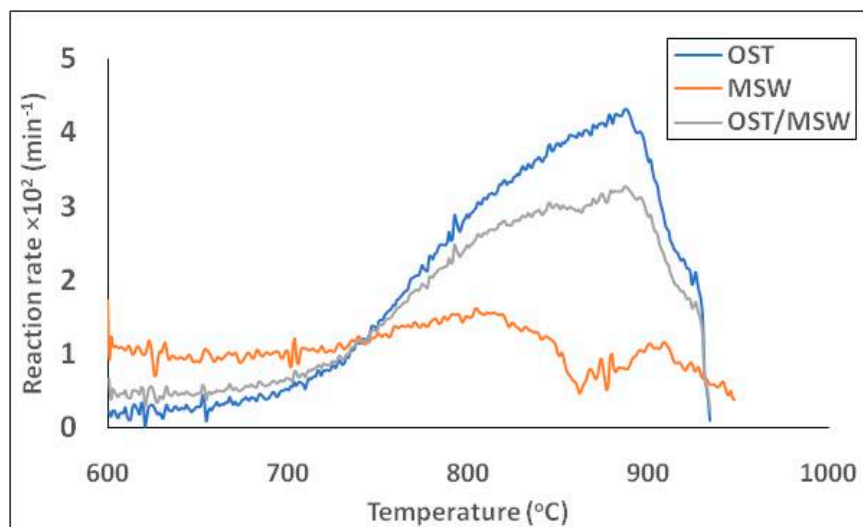


Figure 3. DTG gasification profiles of OST and MSW biochars and their mixture under an atmosphere of carbon dioxide (RSD = 0.2–0.8%).

Table 5. Gasification characteristics of fuels under carbon dioxide atmosphere.

	OST	MSW	OST/MSW
T_i (°C)	650	710	660
T_{max} (°C)	887	805	860
$R_{max} \times 10^2$ (min ⁻¹)	4.4	1.6	3.4
R_{max}/T_{max} (10 ⁴ /min°C)	0.5	0.2	0.4
Gas (mol%)			
CO	94.6	98.0	96.8
H ₂ O	3.1	0.2	2.1
H ₂	2.0	1.2	0.6
CH ₄	0.1	0.3	0.2
C _x H _y	0.2	0.3	0.3
Conversion (%)	83.9	50.1	73.1
Syngas yield (m ³ /kg)	0.75	0.44	0.65

As previously discussed in the introduction section, the most important factors affecting the gasification reactivity are the physical and chemical structure of the chars, as well as inherent potassium and sodium alkali metals. Although OST biochar presented a lower specific surface area than MSW biochar, it had a much lower ash content, higher potassium and sodium concentrations (39.8 g/kg as compared to 16.3 g/kg for MSW) [5] and increased aromaticity, according to the FTIR spectra shown above. These could explain the enhanced reactivity and conversion of this fuel, as compared to MSW material.

Concerning the composition of the gas produced, Table 5 indicates that this consisted principally of CO, i.e., the product of the Boudouard reaction (3). The minor amounts of H₂, H₂O, CH₄ and C_xH_y were generated through reactions (1), (5) and reverse (6). The yield of syngas produced, being directly related to the composition of gas and the final conversion, was 0.75 m³/kg for OST, as opposed to 0.44 m³/kg for MSW. A pyro-gasification study of MSW using carbon dioxide as the gasifying agent showed a yield of 0.71 m³/kg; however, the reactor design was different [45].

3.4. Comparison

By comparing the results of Tables 4 and 5, it can be noticed that gasification efficiency in terms of conversion, under steam with steam/biochar = 3 or under carbon dioxide, was about the same for the fuels studied. Furthermore, as Figure 4 shows, the higher heating value of generated gas was higher when the gasifying agent was carbon dioxide and

practically the same for both materials and their mixture, as the main gas component was CO. Therefore, for MSW fuel, which generated almost the same volume of syngas under a steam and carbon dioxide atmosphere, the overall heat was higher when this was gasified by carbon dioxide. However, the increased syngas yield of OST under steam compensated the lower heating value of gas in this case, so that the overall heat was higher when the gasifying agent was steam. This trend was also observed for the blend of the two materials.

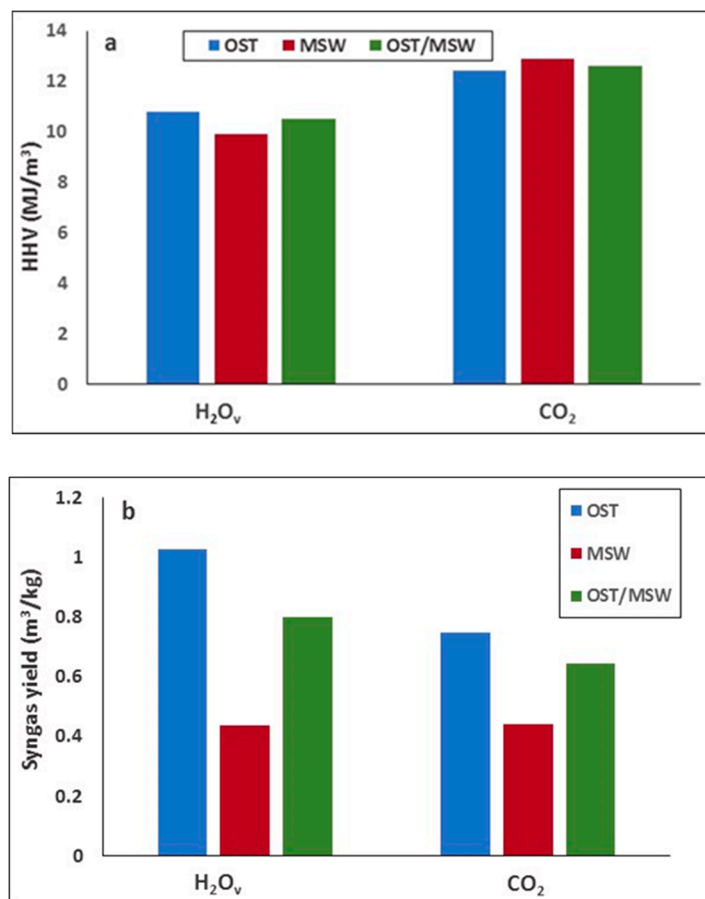


Figure 4. Comparison of (a) heating value and (b) syngas yield from the gasification of the fuels.

4. Conclusions

When gasification was conducted under a steam atmosphere, the concentrations of H₂ and CO₂ in the product gas mixture increased with steam/biochar ratio, while that of CO decreased. The Boudouard reaction was less favored in the case of MSW fuel. At steam/biochar = 3, H₂ yield, higher heating value and conversion were 52.8%, 10.8 MJ/m³ and 87.5%, respectively, for OST biochar; 44.4%, 9.9 MJ/m³ and 51.5% for MSW biochar; and 50%, 10.6 MJ/m³ and 76.6% for their blend.

When gasification was conducted under a carbon dioxide atmosphere, the reactivity and conversion of OST biochar (84%) were significantly higher compared with MSW biochar (50%), due to its higher alkali content and aromaticity, while a lower amount of ash was present. The higher heating value of product gas was 12.4–12.9 MJ/m³. The gasification parameters of the OST/MSW mixture remained close to the weighted average values.

Co-gasification of MSW biochar with OST biochar (at a ratio of 30:70) resulted in enhanced reactivity, conversion, syngas yield and heating value of product gas compared with gasification of solely MSW material.

Author Contributions: Conceptualization, D.V.; software, P.T.; validation, D.V. and P.T.; investigation, D.V.; data curation, P.T.; writing—original draft preparation, D.V.; writing—review and editing, D.V. All authors have read and agreed to the published version of the manuscript.

Funding: This research received no external funding.

Data Availability Statement: Data are contained within the article.

Acknowledgments: The authors kindly thank the laboratories of Hydrocarbons Chemistry and Ore Processing and Beneficiation of the Technical University of Crete for the ultimate and FTIR analyses and BET measurements of the samples, respectively.

Conflicts of Interest: The authors declare no conflict of interest.

Appendix A

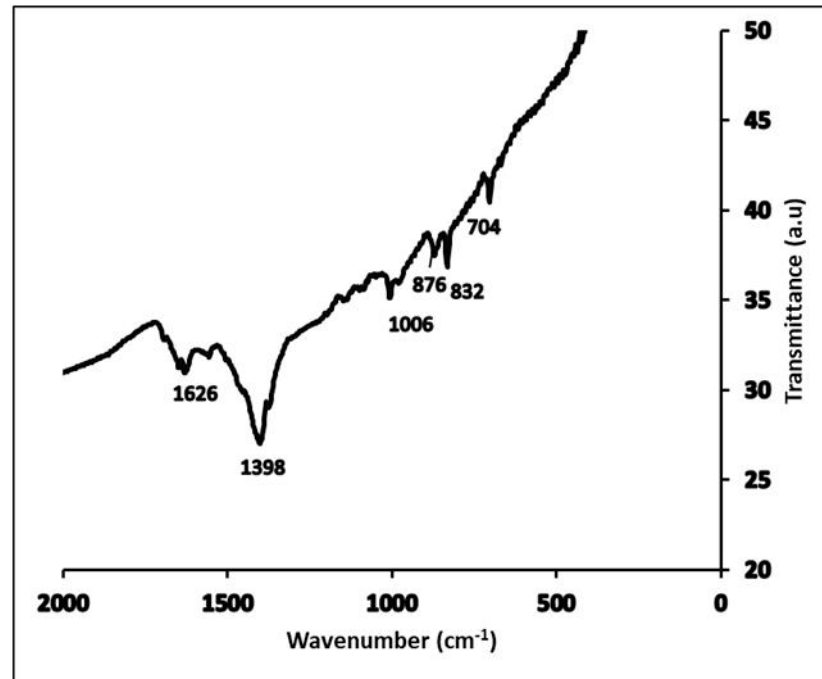


Figure A1. FTIR spectra of OST biochar.

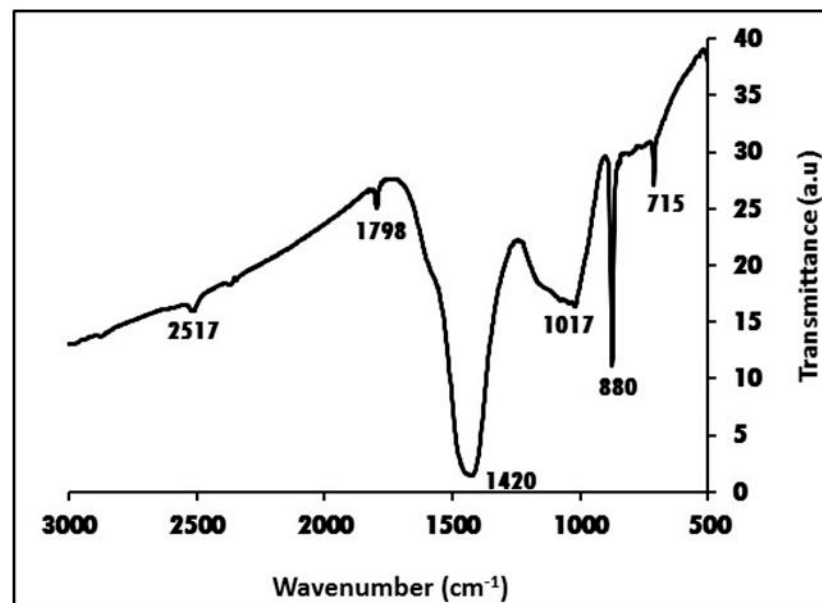


Figure A2. FTIR spectra of MSW biochar.

References

1. Sipra, A.T.; Gao, N.; Sarwar, H. Municipal solid waste (MSW) pyrolysis for biofuels production: A review of effects of MSW components and catalysts. *Fuel Process. Technol.* **2018**, *175*, 131–147. [\[CrossRef\]](#)
2. Wienchol, P.; Korus, A.; Szlek, A.; Ditaranto, M. Thermogravimetric and kinetic study of thermal degradation of various types of municipal solid waste (MSW) under N₂, CO₂ and oxy-fuel conditions. *Energy* **2022**, *248*, 123573. [\[CrossRef\]](#)
3. Liobikiene, G.; Burkus, M. The European Union possibilities to achieve targets of Europe 2020 and Paris agreement climate policy. *Renew. Energy* **2017**, *106*, 290–309.
4. Vamvuka, D. *Biomass, Bioenergy and the Environment*; Tziolas Publications: Salonica, Greece, 2009.
5. Vamvuka, D.; Sfakiotakis, S.; Mpoumpouris, A. Slagging and fouling propensities of ashes from urban and industrial wastes. *Rec. Innov. Chem. Eng.* **2018**, *11*, 145–158.
6. Zaini, I.N.; Lopez, C.G.; Pretz, T.; Yang, W.; Jonsson, P.G. Characterization of pyrolysis products of high-ash excavated-waste and its char gasification reactivity and kinetics under a steam atmosphere. *Waste Manag.* **2019**, *97*, 149–163. [\[CrossRef\]](#)
7. Sajid, M.; Raheem, A.; Ullah, N.; Asim, M.; Rehman, M.S.U.; Ali, N. Gasification of municipal solid waste: Progress, challenges and prospects. *Renew. Sustain. Energy Rev.* **2022**, *168*, 112815. [\[CrossRef\]](#)
8. Wang, B.; Gupta, R.; Bei, L.; Wan, Q.; Sun, L. A review on gasification of municipal solid waste (MSW): Syngas production, tar formation, mineral transformation and industrial challenges. *Int. J. Hydrogen Energy* **2023**, *48*, 26676–26706. [\[CrossRef\]](#)
9. Vamvuka, D.; Alexandrakakis, S.; Papagiannis, I. Evaluation of Municipal Wastes as Secondary Fuels through Co-combustion with Woody Biomass in a Fluidized Bed Reactor. *J. Energy Inst.* **2020**, *93*, 272–280. [\[CrossRef\]](#)
10. Lampropoulos, A.; Kaklidis, N.; Athanasiou, C.; Montes-Morán, M.A.; Arenillas, A.; Menéndez, J.A.; Binas, V.D.; Konsolakis, M.; Marnellos, G.E. Effect of olive kernel treatment (torrefaction vs. slow pyrolysis) on the physicochemical characteristics and the CO₂ or H₂O gasification performance of as-prepared biochars. *Int. J. Hydrogen Energy* **2021**, *46*, 29126–29141. [\[CrossRef\]](#)
11. Bhoi, P.R.; Huhnke, R.L.; Kumar, A.; Indrawan, N.; Thapa, S. Co-gasification of municipal solid waste and biomass in a commercial scale downdraft gasifier. *Energy* **2018**, *163*, 513–518. [\[CrossRef\]](#)
12. Inayat, M.; Sulaiman, S.A.; Kurnia, J.C.; Shahbaz, M. Effect of various blended fuels on syngas quality and performance in catalytic co-gasification: A review. *Renew. Sustain. Energy Rev.* **2019**, *105*, 252–267. [\[CrossRef\]](#)
13. Situmorang, Y.A.; Zhao, Z.; Chaihad, N.; Wang, C.; Anniwaer, A.; Kasai, Y.; Abudula, A.; Guan, G. Steam gasification of co-pyrolysis chars from various types of biomass. *Int. J. Hydrogen Energy* **2021**, *46*, 3640–3650. [\[CrossRef\]](#)
14. Vamvuka, D.; Sfakiotakis, S. Gasification reactivity and mass spectrometric analysis of gases of energy crop chars under a CO₂ atmosphere. *Energy Fuels* **2015**, *29*, 3215–3223. [\[CrossRef\]](#)
15. Hla, S.S.; Lopes, R.; Roberts, D. The CO₂ gasification reactivity of chars produced from Australian municipal solid waste. *Fuel* **2016**, *185*, 847–854. [\[CrossRef\]](#)
16. Ramos, A.; Monteiro, E.; Silva, V.; Rouboa, A. Co-gasification and recent developments on waste-to-energy conversion: A review. *Renew. Sustain. Energy Rev.* **2018**, *81*, 380–396. [\[CrossRef\]](#)
17. Santos, R.G.; Alencar, A.C. Biomass-derived syngas production via gasification process and its catalytic conversion into fuels by Fischer Tropsch synthesis: A review. *Int. J. Hydrogen Energy* **2020**, *45*, 18114–18132. [\[CrossRef\]](#)
18. Hameed, Z.; Aslam, M.; Khan, Z.; Maqsood, K.; Atabani, A.E.; Ghauri, M.; Khurram, M.S.; Rehan, M.; Nizami, A.S. Gasification of municipal solid waste blends with biomass for energy production and resources recovery: Current status, hybrid technologies and innovative prospects. *Renew. Sustain. Energy Rev.* **2021**, *136*, 110375. [\[CrossRef\]](#)
19. Vamvuka, D.; Sfakiotakis, S.; Pantelaki, O. Evaluation of gaseous and solid products from the pyrolysis of waste biomass blends for energetic and environmental applications. *Fuel* **2019**, *236*, 574–582. [\[CrossRef\]](#)
20. Cabuk, B.; Duman, G.; Yanik, J.; Olgun, H. Effect of fuel blend composition on hydrogen yield in co-gasification of coal and non-woody biomass. *Int. J. Hydrogen Energy* **2020**, *45*, 3435–3443. [\[CrossRef\]](#)
21. Vamvuka, D.; Teftiki, A.; Sfakiotakis, S. Increasing the reactivity of waste biochars during their co-gasification with carbon dioxide using catalysts and bio-oils. *Thermochim. Acta* **2021**, *704*, 179015. [\[CrossRef\]](#)
22. Vamvuka, D.; Teftiki, A.; Sfakiotakis, S. Investigating the valorisation of refused derived fuel for energetic uses through its co-gasification with woody wastes. *World J. Environ. Biosci.* **2022**, *11*, 37–44. [\[CrossRef\]](#)
23. Suhaj, P.; Haydary, J.; Husar, J.; Steltenpohl, P.; Supa, I. Catalytic gasification of refuse-derived fuel in a two-stage laboratory scale pyrolysis/gasification unit with catalyst based on clay minerals. *Waste Manag.* **2019**, *85*, 1–10. [\[CrossRef\]](#)
24. Bouraoui, Z.; Jeguirim, M.; Guizani, C.; Limousy, L.; Dupont, C.; Gadiou, R. Thermogravimetric study on the influence of structural, textural and chemical properties of biomass chars on CO₂ gasification reactivity. *Energy* **2015**, *88*, 703–710. [\[CrossRef\]](#)
25. Dupont, C.; Jacob, S.; Marrakchy, K.O.; Hognon, C.; Gâteau, M.; Labalette, F.; Da Silva Perez, D. How inorganic elements of biomass influence char steam gasification kinetics. *Energy* **2016**, *109*, 430–435. [\[CrossRef\]](#)
26. Aluri, S.; Syed, A.; Flick, D.W.; Muzzy, J.D.; Sievers, C.; Agrawal, P.K. Pyrolysis and gasification studies of model refuse derived fuel (RDF) using thermogravimetric analysis. *Fuel Process. Technol.* **2018**, *179*, 154–166. [\[CrossRef\]](#)
27. Lin, C.L.; Weng, W.C. Effects of different operating parameters on the syngas composition in a two-stage gasification process. *Renew. Energy* **2017**, *109*, 135–143. [\[CrossRef\]](#)
28. Islam, M.W. Effect of different gasifying agents (steam, H₂O₂, oxygen, CO₂ and air) on gasification parameters. *Int. J. Hydrogen Energy* **2020**, *45*, 31760–31774. [\[CrossRef\]](#)

29. Chen, G.; Jamro, I.A.; Samo, S.R.; Wenga, T.; Baloch, H.A.; Yan, B.; Ma, W. Hydrogen-rich syngas production from municipal solid waste gasification through the application of central composite design: An optimization study. *Int. J. Hydrogen Energy* **2020**, *45*, 33260–33273. [[CrossRef](#)]
30. Cai, J.; Zeng, R.; Zheng, W.; Wang, S.; Han, J.; Li, K.; Luo, M.; Tang, X. Synergistic effects of co-gasification of municipal solid waste and biomass in fixed-bed gasifier. *Process Saf. Environ. Prot.* **2021**, *148*, 1–12. [[CrossRef](#)]
31. Zhao, J.; Xie, D.; Wang, S.; Zhang, R.; Wu, Z.; Meng, H.; Chen, L.; Wang, T.; Guo, Y. Hydrogen-rich syngas produced from co-gasification of municipal solid waste and wheat straw in an oxygen-enriched air fluidized bed. *Int. J. Hydrogen Energy* **2021**, *46*, 18051–18063. [[CrossRef](#)]
32. Klein, A.; Themelis, N.J. Energy recovery from municipal solid wastes by gasification. In Proceedings of the 11th North American Waste-to-Energy Conference, Tampa, FL, USA, 28–30 April 2003.
33. Cao, Y.; Fu, L.; Mofrad, A. Combined-gasification of biomass and municipal solid waste in a fluidized bed gasifier. *J. Energy Inst.* **2019**, *92*, 1683–1688. [[CrossRef](#)]
34. Lee, U.; Chung, J.N.; Ingle, H.A. High-temperature steam gasification of municipal solid waste, rubber, plastic and wood. *Energy Fuels* **2014**, *28*, 4573–4587. [[CrossRef](#)]
35. Zheng, X.; Ying, Z.; Wang, B.; Chen, C. Hydrogen and syngas production from municipal solid waste (MSW) gasification via reusing CO₂. *Appl. Therm. Eng.* **2018**, *144*, 242–247. [[CrossRef](#)]
36. Irfan, M.; Li, A.; Zhang, L.; Wang, M.; Chen, C.; Khushk, S. Production of hydrogen enriched syngas from municipal solid waste gasification with waste marble powder as a catalyst. *Int. J. Hydrogen Energy* **2019**, *44*, 8051–8061. [[CrossRef](#)]
37. Kwon, E.; Westby, K.J.; Castaldi, M.J. Transforming municipal solid waste MSW into fuel via the gasification/pyrolysis process. In Proceedings of the 18th Annual North American Waste to Energy Conference ASME, Orlando, FL, USA, 11–13 May 2010.
38. Vamvuka, D.; Karouki, E.; Sfakiotakis, S. Gasification of waste biomass chars by carbon dioxide via thermogravimetry-Effect of catalysts. *Combust. Sci. Technol.* **2012**, *184*, 64–77. [[CrossRef](#)]
39. Gonzalez-Vazquez, M.P.; Garcia, R.; Gil, M.V.; Pevida, C.; Rubiera, F. Unconventional biomass fuels for steam gasification: Kinetic analysis and effect of ash composition on reactivity. *Energy* **2018**, *155*, 426–437. [[CrossRef](#)]
40. Prestipino, M.; Galvagno, A.; Karlstrom, O.; Brink, A. Energy conversion of agricultural biomass char: Steam gasification kinetics. *Energy* **2018**, *161*, 1055–1063. [[CrossRef](#)]
41. CEN/TC 335; Solid Biofuels. Available online: <https://standards.iteh.ai/catalog/tc/cen/9b867592-e942-4916-b3c4-8a2840e0429f/cen-tc-335> (accessed on 10 December 2023).
42. Eshun, J.; Wang, L.; Ansah, E.; Shahbazi, A.; Schimmel, K.; Kabadi, V.; Aravamudhan, S. Characterization of the physicochemical and structural evolution of biomass particles during combined pyrolysis and CO₂ gasification. *J. Energy Inst.* **2019**, *92*, 82–93. [[CrossRef](#)]
43. Zhai, M.; Zhang, Y.; Dong, P.; Liu, P. Characteristics of rice husk char gasification with steam. *Fuel* **2015**, *158*, 42–49. [[CrossRef](#)]
44. Li, W.; Wu, S.; Wu, Y.; Huang, S.; Gao, J. Gasification characteristics of biomass at a high-temperature steam atmosphere. *Fuel Process. Technol.* **2019**, *194*, 106090. [[CrossRef](#)]
45. Ge, S.; Tahir, M.H.; Chen, D.; Hong, L.; Feng, Y.; Huang, Z. MSW pyro-gasification using high-temperature CO₂ as gasifying agent: Influence of contact mode between CO₂, char and volatiles on final products. *Waste Manag.* **2023**, *170*, 112–121. [[CrossRef](#)]

Disclaimer/Publisher’s Note: The statements, opinions and data contained in all publications are solely those of the individual author(s) and contributor(s) and not of MDPI and/or the editor(s). MDPI and/or the editor(s) disclaim responsibility for any injury to people or property resulting from any ideas, methods, instructions or products referred to in the content.